

# Bio-based superabsorbent hydrogels for nutrient-controlled release

Alessandra B. Ribeiro<sup>1\*</sup>, Helena Moreira<sup>1</sup>, Sofia I.A. Pereira<sup>1</sup>, Mariana Godinho<sup>1</sup>, Paula Castro<sup>1</sup>, Carla F. Pereira<sup>1</sup>, Francisca Casanova<sup>1</sup>, Ricardo Freixo<sup>1</sup>, Manuela E. Pintado<sup>1</sup>, Óscar L. Ramos<sup>1</sup>

<sup>1</sup> Universidade Católica Portuguesa, CBQF - Centro de Biotecnologia e Química Fina – Laboratório Associado, Escola Superior de Biotecnologia, Rua Diogo Botelho 1327, 4169-005 Porto, Portugal.

\* Corresponding author: email: [abriereiro@ucp.pt](mailto:abriereiro@ucp.pt)

## Abstract

The drought is characterized by a low water precipitation rate, with strong impact on the crop productivity, threaten global food production. In this context, the use of soil amendments, such as superabsorbent hydrogels constitute a potential technology for water use efficiency and increase crop yields. In this work, it was synthesised a cellulose-based hydrogel, carrying out its characterisation, evaluated its environmental safety and its potential to be used as a soil amendment. The hydrogel was successfully synthesised using a simple process and inexpensive reagents. The hydrogel showed pH of 6.0 to 7.5 and conductivity below 10.0  $\mu\text{S cm}^{-1}$ . The FTIR showed a low intensity peak in the crystallinity region, which was supported by the low crystallinity index ( $27.3\% \pm 0.6$ ) verified by PXRD analysis. The swelling capacity reached more than 200 g of water, the hydrogel showed good resistance to osmotic pressure and high thermostability, which favours the application in hot and arid areas. Regarding the safety evaluation, no potentially hazardous compound was detected, nor was there any adverse effect on soil microorganisms. In addition, the hydrogel was found to be safe for use during sowing and for promoting seedling development. In the green pot experiment, the hydrogel demonstrated a significant increase in maize biomass, root biomass and potential to serve as a reservoir for soil nutrients. In conclusion, the superabsorbent hydrogel exhibited promising characteristics for use as a soil amendment, scalability potential and constitutes a sustainable alternative for agricultural applications.

**Keywords:** nutrient release; biopolymers; hydrogels; crop production; drought; soil amendment; bio-based materials; delivery systems; agriculture.

## 1. Introduction

Water scarcity is a major environmental problem that has been exacerbated in the last decades by climate change [1]. Drought is among the worst natural disasters that occur in the world, characterized by a low water precipitation rate. Its effects have far-reaching consequences, causing severe impacts on human health, economy, and agriculture [2]. More than 50 million people have been suffering the consequences of droughts every year around the globe [2]. Besides, several countries are facing more frequent and severe droughts, which seriously hamper crop productivity and threaten the sustainability of agriculture and food production worldwide [3]. Indeed, 83 % of damages and losses caused by drought directly affect agriculture [4]. In the last 40 years, the number of plants affected by droughts doubled, with a significant reduction in the production of the main crops (e.g., 40 % in maize production). Additionally, almost 12 million hectares of land have been lost each year due to water scarcity [5–7].

Under this context, it became mandatory and urgent to develop water-saving strategies in the agricultural sector. These strategies are essential for the sustainable and efficient management of water resources, allowing the production of more food, while using less land and water [7]. One of the strategies to mitigate the problems related to drought is the use of soil amendments [8]. In this regard, the use of superabsorbent hydrogels (SAP) constitutes a potential technology for improving water use efficiency in agricultural soils and increasing crop yields [9–11]. The SAP are synthesized, aiming a high-water absorption and retention into their three-dimensional networks. A global meta-analysis concluded that SAP effectively improves crucial parameters in plant cultivation, such as growth and yield of various crops, namely wheat, maize, rice, soybean, and cotton [12].

Natural and biopolymers have been explored for SAP synthesis. For instance, El-Aziz et al. (2022) [13] used a pectin and starch-based hydrogel in a greenhouse experiment for tomato fruit production, and Mazloom et al. (2020) [6] explored a lignin-based hydrogel as a soil additive in maize cultivation. However, the commercially available hydrogels are mostly synthetic or semi-synthetic, based on acrylic acid or acrylamide, which can present environmental issues if not disposed of properly. Some of these products include the Pusa hydrogel, which consists of a derivatized cellulose-grafted-anionic polyacrylate product; and Alsta Hydrogel, Polyter<sup>®</sup>, TrueHydrogel<sup>®</sup> and SocoPolymer<sup>®</sup>, which are potassium

polyacrylate derivative hydrogels. Therefore, due to their chemical composition, it is highly recommended the replacement of this type of hydrogels by greener substitutes [14,15].

The analysis of 129 articles concerning natural and synthetic SAP for agricultural application demonstrated that these two types of hydrogels improved the crop yield in a similar way. However, natural hydrogels were presented as lower-cost alternatives with reduced time of biodegradation, suggesting the potential of natural SAP to dominate the market in the near future [16]. The SAP based on polymers from waste or by-products have been indicated as promising products since they are readily available, cheap, environmentally sustainable, biodegradable and promote circular economy in agriculture [17,18]. Among the natural polymers used to synthesize hydrogels, cellulose is the most abundant natural polysaccharide found in waste and by-products. Cellulose advantages include biodegradability, non-toxicity, biocompatibility, and low cost [19]. Thus, the development of hydrogel using cellulose from by-products, such as sugarcane bagasse, presents several beneficial aspects. These advantages include the eco-friendly synthesis process, a sustainable approach due to the use of renewable starting materials, and the possibility of becoming a greener alternative to synthetic hydrogels. In addition to their water absorption and retention capabilities, SAP enables the incorporation of nutrients. Among the nutrients that could exert additional benefits to crop production, the main three are nitrogen (N), phosphorus (P), and potassium (K), being the first with the highest demand for plants. As a source of N, urea is the most important commercialized compound, since present high N concentration, is safe, easy to transport, and shows proper stability [20,21]. In this way, cellulose-based hydrogels loaded with urea could be used as an environmentally friendly N fertilizer and a water source for drought-affected areas, reducing the urea pollution in the field and protecting the water resources.

The most reported SAP for agricultural application are complex and present a multi-step reaction synthesis, as oxidation, irradiation, and chemical cross-linking [16,22]. However, authors rarely report the evaluation of the remaining residues from reaction or any other environmental safety assessment. Additionally, just few articles report the effect of the hydrogel application on the soil bacterial community [23,24]. The use of synthetic hydrogels can lead to modifications in the physicochemical characteristics and an increase of soil salinization, which could affect the soil microbiome [24]. Even though, there is a limited number of articles describing the impact of hydrogels on soil physical properties [25].

Considering the lack of a complete study of cellulose-based SAP, the present work aimed to perform a detailed description of the hydrogel synthesis to be used as a soil amendment for maize growth under different irrigation regimes in a greenhouse experiment. This includes the loading of nutrients, the detection of potential undesired compounds from the synthesis reaction, and their effects on seed germination and soil bacteria. By conducting this study, it will be possible to understand the bottleneck of hydrogel production, address concerns regarding the presence of undesired compounds, and explore the beneficial effects of natural SAP on plant growth compared to synthetic counterparts.

## **2. Material and Methods**

### **2.1. Chemicals**

The reagents carboxymethylcellulose (CMC), cellulose, urea, hydrogen peroxide and epichlorohydrin were purchased from Sigma-Aldrich (St. Louis, MO, USA); sulfuric acid and sodium chloride were purchased from Fluka (Steinheim, Germany); sodium hydroxide and citric acid monohydrated were purchased from LabChem (Pennsylvania, USA). The Celluclast<sup>®</sup> 1.5 L was purchased from Novozymes (Norway). Phosphate buffer saline tablets Dulbecco A (PBS), Nutrient broth (NB) and Muller Hinton Agar (MHA) were purchased from Oxoid (England). All chemicals were analytical-grade and used without further purification. Polyter<sup>®</sup> was purchased to Green Tech Novation company (France).

### **2.2. Synthesis of hydrogels**

For the hydrogel synthesis, the cellulose was solubilized in NaOH/urea solvent system and mixed with epichlorohydrin, used as crosslinker, under mechanical stirring conditions referred in Table 1. The solutions were then kept overnight for hydrogels curing. To remove any non-reactant compounds, the hydrogels were exhaustively washed with deionized water and then kept in acidified water (pH 3-4) overnight to reach a final pH between 6-7, and a maximum conductivity of 10  $\mu\text{S cm}^{-1}$ . Afterwards, the hydrogels were dried at 50-60 °C using a vacuum oven, after its desiccation in phase inversion induced by the sample immersion in ethanol 96 % (v v<sup>-1</sup>) for 2 hours at room temperature (20-25 °C) [26].

Table 1. Reaction conditions and chemical composition of the cellulose-based hydrogels.

Hydrogel	Raw material	Solvent system	Crosslinker	Conditions
H1	<b>Formulation 1:</b> CMC (3 wt.%) + Cellulose from bagasse (autohydrolysis + bleaching) (3 wt.%) (9:1, w/w)	NaOH (7 %, w/v) Urea (12 %, w/v)	Epichlorohydrin (7.5 %, v/v)	200 rpm/60 °C/ 1h 60 °C/ 24h
H2	<b>Formulation 2:</b> CMC (3 wt.%) + Commercial cellulose (Sigma-Aldrich) (3 wt.%) (9:1, w/w)	NaOH (7 %, w/v) Urea (12 %, w/v)	Epichlorohydrin (7.5 %, v/v)	200 rpm/60 °C/ 1h 60 °C/ 24h

The hydrogel yield was calculated considering the quantity of each reagent used in the initial synthesis and the total mass obtained after the curing period [27], following the Eq A1:

Eq. A1:

## 2.3. Hydrogel Characterization

### 2.3.1. Biophysical properties

#### pH/conductivity

The pH and electrical conductivity of hydrogels were measured at 22 °C using a portable benchtop pH/conductivity meter (Meter S210, Mettler Toledo Seven Compact™, Japan). The measurements were conducted in triplicate.

#### Optical properties

The absorbance spectra of hydrogels were measured from 250 to 800 nm on an UV-visible spectrometer (Shimadzu model UV-1900, Japan) equipped with deuterium and tungsten lamps from 200 to 900 nm. The transparency-opacity of hydrogels was verified in the maximum wavelength ( $\lambda$ ) detected in the spectrum [28]. The measurements were conducted in triplicate.

#### Tensile strength

The tensile strength of hydrogels was evaluated resorting to a Texture Analyzer TA.XT plus (Stable Micro System, London, UK) using a cylinder probe (P/0.5R; contact area: 126.68 mm<sup>2</sup>) and compression test mode. The test was conducted with pre-test and test speed of 1.0 mm

s<sup>-1</sup>, post-test speed of 100 mm s<sup>-1</sup>, and 5 mm of distance target and 500 pps of data acquisition rate. The measurements were conducted in triplicate.

### **2.3.1. Morphological properties**

The appearance and morphology of hydrogels were evaluated through an optical microscope (AxioLab A1-Carl Zeiss, Germany) in contrast mode and images were recorded with a digital camera (AxioCam 305 color). The measurements were conducted in duplicate. In addition, the microstructure of hydrogels was evaluated resorting to Scanning Electron Microscope (SEM) (JSM-5600 LV from JEOL, Japan). Prior to analysis, the dried samples were placed in observation stubs (covered with double-sided adhesive carbon tape (NEM tape, Nisshin, Japan) and coated with Aug/Pd using a Sputter Coater (Polaron, Bad Schwalbach, Germany). All observations were performed in high-vacuum with an acceleration voltage of 20 kV, at a working distance of 18-19 mm and a spot-size of 4. The measurements were conducted at least in duplicate.

### **2.3.2. Structural properties**

#### **FT-IR spectroscopy**

The FT-IR spectra of each hydrogel was recorded using the Frontier™ MIR/FIR spectrometer from PerkinElmer (Massachusetts, USA) in a scanning range of 550-4000 cm<sup>-1</sup> for 16 scans at a spectral resolution of 4 cm<sup>-1</sup>. All analyses were done in triplicate.

#### **Powder X-Ray Diffraction Analysis**

Powder X-Ray Diffraction Analyses (PXRD) were performed on Rigaku MiniFlex 600 diffractometer with Cu K $\alpha$  radiation, with a voltage of 40 kV and a current of 15 mA ( $3^\circ \leq 2\theta \leq 60^\circ$ ; step of 0.01 and speed rate of 3.0 °C min<sup>-1</sup>).

#### **Rheological assessment**

The storage ( $G'$ ) and loss ( $G''$ ) moduli of hydrogels were calculated using a controlled stress rheometer model CS-50 (Bohlin Instruments, Cranbury NJ, USA), equipped with a Peltier system for temperature control, using a cone-plate geometry of 4°/40mm (rotating plate diameter of 40 mm, and gap of 150  $\mu$ m). Testing was made at low strain amplitude (0.05 %) and low frequency (0.01-10 Hz) at isothermal mode at 25 °C, within the linear viscoelastic range — as assessed by stress and frequency sweep experiments.

### 2.3.3. Thermal properties

#### Differential Scanning Calorimetry

Thermal analyses were performed resorting to a Differential Scanning Calorimeter (DSC) (204 F1 Phoenix®, NETZSCH-Gerätebau GmbH). Calibration of temperature and enthalpy scale was carried out using an indium/zinc standard. Hydrogels (i.e., weight of ca. 3–5 mg) and reference (i.e., empty pan) were hermetically sealed, with pierced lids, and heated in aluminum pans over a range of 25–500 °C at a constant rate of 10 °C min<sup>-1</sup>. The inert atmosphere was maintained by purging nitrogen gas at a flow rate of 40 mL min<sup>-1</sup>.

#### Thermogravimetry

Thermogravimetric analyses (TGA) were performed with a STA 449 F5 Jupiter (NETZSCH-Gerätebau GmbH). The samples were placed in the balance system and heated from 30 to 1550 °C at 10 °C min<sup>-1</sup>, under nitrogen atmosphere. The samples were pre-weighed (10 mg) in aluminum pans using an empty pan as reference. The initial decomposition temperature (T<sub>di</sub>), the derivate maximum decomposing rate temperature (DTG<sub>max</sub>) and the corresponding weight loss, as well as the residual mass were all determined. The measurements were performed in duplicate.

### 2.3.4. Functional properties

#### Swelling in deionized water

The water absorption of hydrogels was determined as follows: ca. 100 mg (W<sub>d</sub>) of each hydrogel was placed into the tea bag nylon and then immersed in deionized water (pH between 6.0-6.5 and conductivity between 0.8-1.5 μS cm<sup>-1</sup>) at 25 °C. After 24 h, the hydrogel was removed from water, and the excess of solvent was gently drained with a paper towel and the mass was weighted (W<sub>h</sub>). The water absorption was calculated using the Eq. A2:

Eq. A2

#### Swelling affected by salinity

Dried hydrogels (30-50 mg) were weighted (W<sub>d</sub>) and placed in contact with salt solutions (200 mL of 0.1 M NaCl, KCl and Na<sub>2</sub>SO<sub>4</sub>). The mixture was kept for 72 h at room temperature (20-25 °C) without mechanical agitation, after this time, the excess of salt solution was drained.

The hydrogel was weighted ( $M_h$ s) and dried at 50 °C until constant weight. The swelling capacity of dried hydrogel in the presence of salt solution was calculated using the Eq. A3:

Eq. A3

### **Water absorption in loam and sandy soil**

The water absorption of hydrogels in the presence of a loam and sandy soil, simulating their use in agriculture, was performed according to EN 1097-6: 2022 [29] with some modifications. Briefly, ca. 30 mg of grounded dried hydrogel was mixed with 30 g of loam and sandy soil (dried at 105 °C until constant weight). The dried mixture of soil and hydrogel ( $M_d$ ) was fully immersed in 25 mL of deionized water (pH 7.0, conductivity 0.7  $\mu\text{S cm}^{-1}$ ) for 24 h at room temperature without agitation. After this period, the mixture was filtered using a vacuum system. Loam and sandy soils without hydrogel were used as a negative control, while a commercial water retainer product - Polyter® - was used as positive control. The hydrated mixture ( $M_h$ ) was weighted, and the water absorption was calculated following Eq A4:

Eq. A4:

### **Loading capacity**

The capacity of hydrogels to load urea was determined for 72 h as follows: ca. 50 mg of dry hydrogel ( $M_h$ ) was weighted and placed in contact with 200 mL of urea solution (5 %, w/v), for 72 h at room temperature. Then, the excess of urea was drained, and the hydrogel was rinsed with deionized water to remove unreacted urea. After this step, the hydrated hydrogel was weighted ( $M_{hu}$ ) and dried at 50 °C until constant weight ( $M_{hud}$ ) [30]. The mass of urea absorbed by the hydrogel (g/per gram of dried hydrogel) was calculate using the Eq. A5, while the hydrogel swelling capacity in the presence of urea solution was calculate using the Eq. A6:

Eq. A5:

Eq. A6

## **2.4. Environmental and Biological Safety**

### **2.4.1 Residual epichlorohydrin after hydrogel degradation**



To evaluate the potential release of epichlorohydrin from hydrogel, hydrogels H1 and H2 were enzymatically hydrolyzed and the epichlorohydrin that could be released was quantified by gas chromatography-mass spectrometry (GC-MS). The hydrolysis of the hydrogel base material was carried out according to the procedure described by Kono (2014) [27], with slight modifications. Briefly, about 100 mg of each hydrogel (H1 and H2) was soaked in 19 mL of 25 mM citrate buffer (pH 4.5) for 24 h. The Celluclast® enzymatic preparation was dissolved in 1 mL of the same buffer to obtain the final pH of 4.5, and it was added to the suspension to a final concentration of 10 units/mL. Then, the mixture was incubated at 40 °C for complete hydrogel degradation. The suspension obtained was then used for epichlorohydrin extraction and quantification to verify if any of it was released from the hydrogel matrix. To do so, 200 mL of sample solution was transferred into 500 mL of separation funnel, 10 g of NaCl was added and after the complete salt dissolution, 10 mL of methylene chloride was added. The funnel was shaken for 2 min, kept for 2-5 min for layers separation, and the organic layer was collected. The extraction process was repeated twice with fresh solvent, and the combined organic extracts were concentrated in K-D tube using speed vacuum equipment. The concentrated extracts were dissolved in 1 mL of methylene chloride and analyzed by GC-MS for epichlorohydrin detection, and quantification using the method described by Cai & Zou (2010) [31]. A GC-QqQ model EVOQ (Bruker, Karlsruhe, Germany) mass spectrometer instrument equipped with split capillary system, and Restek Rxi®-5Sil MS, 30 x 0.25 mm, 0.25 µm column were used. The injector was set at 250 °C with a split mode 5:1 using helium as carrier gas at constant flow mode (1 mL min<sup>-1</sup>). The oven temperature started at 30 °C with a hold period of 2 min, then it was raised at 10 °C min<sup>-1</sup> until 100 °C with a hold period of 2 min, and then increased to 120 °C with a hold period of 2 min. The compound identification was based on the information available on the NIST library, and the quantification was performed using an epichlorohydrin calibration curve from 0.001 g L<sup>-1</sup> to 0.5 g L<sup>-1</sup> with correlation coefficient of 0.998. All samples were analyzed in triplicate.

#### **2.4.2 Impact of hydrogels on soil microorganisms**

The potential negative effect of hydrogels on soil microorganisms was evaluated based on the Kirby Bauer susceptibility protocol [32–34]. The agar disk-diffusion method (or Kirby Bauer method) is a well-known method to test the susceptibility of pure culture of microorganisms against a compound or drug [34,35]. All the variables, namely temperature, inoculum size,

and incubation time are standardized, and the qualitative results classified the microorganisms as susceptible, intermediate and resistant in relation to the tested compound or material [34,35]. Pure cultures of five bacterial strains, *Arthrobacter nicotinovorans* EAPAA, *Rhodococcus* sp. EC35, *Bacillus megaterium* ST2-3, *Pseudomonas brassicacearum* ZR 2-4 and *Pseudomonas azotoformans* IR1-11, previously isolated from soil and plant tissues [36–38], were grown in Nutrient Broth overnight at 30 °C, under agitation 120 rpm. The diluted bacterial suspension (i.e., 0.5 McFarland standard) was inoculated in Muller Hinton Agar plates. In parallel, the hydrogels were soaked in sterile Phosphate-Buffered Saline (osmolality 280-315 mOsm Kg<sup>-1</sup>, pH 7.4), the excess of buffer was drained, and the hydrogels were sterilized under UV-radiation for 4 h. About 100 mg of each sterilized hydrogel was gently placed directly on the surface of the previously inoculated MHA plates which were and incubated at 30 °C for 24 h. After this period, the presence of inhibition hale around the hydrogel was verified [32]. All samples were analyzed in duplicate.

#### **2.4.3 Impact of hydrogels loaded with urea on maize seed germination**

Different concentrations of urea (i.e., 0.1, 0.2, 0.5, 1, 2, and 5 %) were pre-screened on maize germination to select the optimal concentration (i.e., the maximum concentration of urea that does not inhibit the maize seed germination) to be loaded in the hydrogels. Therefore, 6 mL of each urea solution or 6 mL of sterile deionized water (used as control) were added to 120 mm square Petri dishes containing a sterilized filter paper (Whatman No. 1). Ten maize seeds (*Zea mays*) var. Deckalb were previously sterilized with 0.5 % (v v<sup>-1</sup>) NaOCl for 10 min, followed by several washes with deionized-sterilized water and then placed in each Petri dish. After 7 days of incubation in the dark, the germination rate, and root and shoot length of maize seedlings were measured. The experiment was performed in triplicate.

The maximum concentration of urea that did not inhibit the maize seed germination was used to load H1 and H2. For this purpose, 25 mL of each hydrated hydrogel (0.02 %) was added to Petri dishes, on which ten maize sterilized seeds were placed. A similar amount of a commercial hydrogel product (Polyter ®) having in its composition some nutrients, namely 0.03 % of magnesium oxide (MgO), 0.5 % of nitrogen (N), 0.2 % of potassium oxide (K<sub>2</sub>O), and 0.8 % of phosphate (Polyter, 2019) was used. Root and shoot length of maize seedlings and

germination rate were determined after 7 days of incubation in the dark at room temperature. The experiment was performed in triplicate.

## **2.5. Greenhouse pot experimental design**

A greenhouse pot experiment was assembled in a controlled growth room (12 h photoperiod, 450  $\mu\text{mol m}^{-1} \text{s}^{-1}$  photosynthetically active radiation, 18–21 °C temperature range, 50–60 % relative humidity range) at Centro de Biotecnologia e Química Fina, Universidade Católica Portuguesa, Porto, Portugal. For the greenhouse experiment a factorial design of 45 experiments comprising 3 hydrogels (H1, H2 and Polyter (P)), 3 irrigation regimes (100 %, 75 %, and 50 % of maize irrigation needs) and 5 replicates was used. The soil used in this study was collected randomly in an agricultural area in northern Portugal (41°10'N, 8°33'W; NW Portugal). The soil properties were as follows: pH (H<sub>2</sub>O) of 6.5; pH (CaCl<sub>2</sub>) of 5.8; conductivity of 0.148 mS cm<sup>-1</sup>; texture loamy-sandy (sand 66 %, clay 18 %, loam 16 %); organic matter content of 5.72 %; total N of 0.27 %; extractable P<sub>2</sub>O<sub>5</sub> of 2581 mg kg<sup>-1</sup>; extractable K<sub>2</sub>O of 122 mg kg<sup>-1</sup>; extractable CaO of 3452 mg kg<sup>-1</sup>; extractable MgO of 134 mg kg<sup>-1</sup>).

Maize seeds were surface sterilized as previously described and germinated in water-agar for 5 days. Three maize seedlings were then transferred and sown in plastic pots containing 500 g of soil or 500 g of soil amended with 0.2 % of hydrogels H1 or H2, both loaded with 0.1 % of urea, or in alternative 0.2 % of Polyter (commercial hydrogel product used as control). After 1 week, seedlings were thinned to 2 per pot.

### **2.5.1 Plant analysis – biometric parameters**

Plants were harvested after 42 days. Shoot elongation was evaluated by measuring the height of each plant. Fresh biomass of shoots and roots was weighted. Dry biomass was determined after oven drying shoots and roots at 65 °C until constant weight.

### **2.5.2 Plant analysis – nutritional parameters**

Shoots and roots were then ground to powder using a grind mill. For nitrogen determination, 150 mg of roots and shoots were weighted and analyzed on the Dumatec™ 8000/FOSS equipment (He flow rate: 195.0 mL min<sup>-1</sup> and O<sub>2</sub> flow rate: 400 mL min<sup>-1</sup>, pressure: 1200 mBar). Ethylenediaminetetraacetic acid (EDTA) was used as a N calibration curve (10.9 mg–

150.2 mg). For the quantification of P and K, ca. 150 mg of each sample was weighed into the Teflon digestion vessel and mixed with 4.5 mL of H<sub>2</sub>SO<sub>4</sub> mL concentrate (98 %) and 4.5 mL of hydrogen peroxide solution (30 %). The suspension was agitated and after 20 min, the vessel was closed and submitted to a cycle at 190 °C for 30 min in a microwave digestion system (Model Speedwave®Xpert, Berghof, Germany). Afterwards, the solution was cooled, transferred to a volumetric flask, and added ultrapure water totaling 25 mL. The final solution was analyzed by an Inductively Coupled Plasma Optical Emission Spectrometry ICP-OES spectrometer (Optima 7000 DV). The total concentrations of N, P and K in the plants were used to calculate the physiological nutrient use efficiency (pNUE) for these elements, according to the Eq. A7 and Eq. A8 [39]:

Eq. A7

Eq. A8

### **2.5.3 Soil analysis**

Soil moisture was assessed at harvest by oven drying 5 g of soil of each pot at 105 °C until constant weight. The pH value and conductivity were determined according to Houba et al. (1955) [40].

### **2.6. Statistical analysis**

Statistical analyses were performed in R Software version 2023.06.0+421. One-way ANOVA with Duncan post hoc analysis was performed to assess the effects of treatments on the different plant parameters. Pearson correlation ( $r$ ) was used to measure the linear dependences between variables.

## **3. Results and Discussion**

### **Synthesis of hydrogels and yield**

The synthesis of cellulose-based hydrogels followed three main steps: the cellulose dissolution, the crosslinking reaction using epichlorohydrin for 3D network formation, and the rinsing with tap water for the hydrogels to reach neutral pH and low conductivity.

Hydrogel 1 (H1) was synthesized using fibers of natural cellulose extracted from sugarcane bagasse. The addition of cellulose fibers improves the mechanical strength of hydrogels favoring their structural stability. This is described as essential for hydrogels to be used as carriers of nutrients, reducing the frequency of its replacement [16]. For comparison purposes, Hydrogel 2 (H2) was synthesized using the same conditions and reagents but a commercial high-pure cellulose from Sigma-Aldrich-Aldrich was used instead of a cellulose from sugarcane bagasse (Table 1). The sugarcane bagasse, the most available by-product of the sugarcane industry, presents a high percentage of polysaccharides, namely cellulose, which can be used to produce hydrogels for different applications. However, the main obstacle is the extraction and efficient solubilization of cellulose. In this way, the method explored to extract cellulose from sugarcane bagasse was the autohydrolysis process at 170 °C for 1 h followed by a bleaching step [41].

Regarding cellulose solubilization, the polymer is insoluble in water and exhibits poor reactivity, mainly due to its strong inter- and intramolecular hydrogen bonds and high degree of crystallinity. Cellulose can be dissolved in the presence of aqueous-alkaline conditions and co-solute (*e.g.*, poly- (ethylene glycol), thiourea, urea) [42]. Urea promotes the weakening of hydrophobic interactions, consequently, enhancing cellulose solubility [43]. Considering that, the dissolution of cellulose fibers was performed using an aqueous NaOH/urea solvent system (Table 1). The alkaline medium based on NaOH/urea proved to be also appropriate for the cellulose-epichlorohydrin crosslinking, since the hydrogel synthesis was successfully achieved resulting in a homogeneous, transparent to slightly opaque hydrogel (Fig. 1). Chemical crosslinking among cellulose and epichlorohydrin was also successfully obtained, leading to a strong and permanent gel-like structure (Fig. 1). This result is in agreement with the results obtained by Palanivelu et al. (2022).

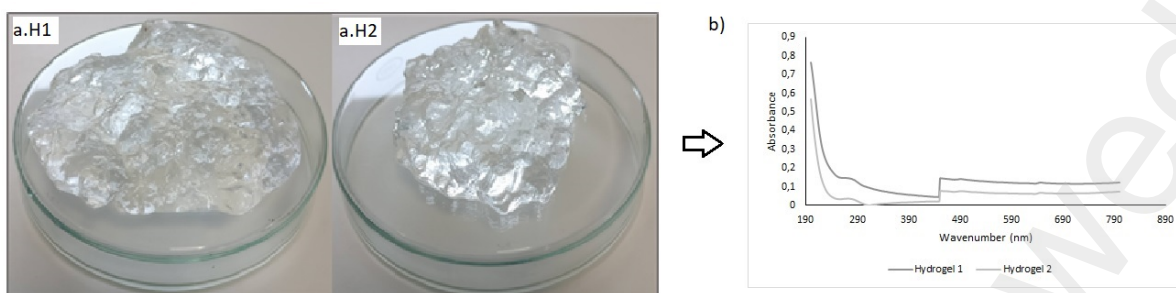


Figure 1. Images of aH1) cellulose-based hydrogel synthesized using natural cellulose fibers extracted from sugarcane bagasse (H1) and of aH2) cellulose-based hydrogel synthesized using commercial cellulose from Sigma-Aldrich (H2). b) Absorbance profile of Hydrogels H1 and H2.

The yield of cellulose hydrogels obtained after the synthesis was  $27.5 \pm 3.4 \%$  and  $29.2 \pm 3.8 \%$  for H1 and H2, respectively. It is important to highlight that the synthesis was performed with a simple process and relatively low-cost reagents, using low-to-moderate temperature (i.e.,  $60 \text{ }^\circ\text{C}$ ) to promote the hydrogel polymerization, thus indicating the scalability potential of this process for industrial production of a competitive product.

## Hydrogels Characterization

### pH and conductivity

The hydrogels, after washing and neutralizing, presented a pH value ranging from 6.0 to 7.5 and a conductivity below  $10.0 \text{ } \mu\text{S cm}^{-1}$ , which is within the safe range parameters for agriculture products. The pH is considered an important factor in the soil microbiome, mainly because bacterial communities present low tolerance to pH variation [44]. Thus, it is crucial to ensure a neutral pH of hydrogels to guarantee that their use will not impact the soil pH. Additionally, the low conductivity values found for both hydrogels indicate the low or even the absence of residual non-reactant compounds, such as NaOH, urea, epichlorohydrin, or its derivatives.

### Optical properties

Through the optical observation of hydrogels (**Error! Reference source not found.**), it was possible to see that H1 and H2 were translucent when hydrated. The high transparency of both H1 and H2 can be verified by the low absorbance recorded between 250-800 nm. Analyzing the optical properties, the maximum absorbance was 0.146 and 0.139 reached at 450 nm and between 240-280 nm, respectively, for H1 and at 0.078 at 450 nm for H2. The

slightly superior absorbance for H1 mainly in the region of 200-280 nm, may be explained by the less purity of cellulose likely due to the presence of lignin traces remaining from the extraction process from sugarcane bagasse. Lignin is reported to present high absorbance in the region between 240 to 280 nm, which is derived from the aromatic ring and the free and etherified hydroxyl groups [45,46].

### **Microscopic evaluation**

Through the optical microscope inspection (**Error! Reference source not found.**), it was possible to observe the presence of small fibers in both hydrogels (H1 and H2), which helps to increase the mechanical strength. Mechanical fragility is one of the main concerns in hydrogels use for agricultural application, since they may have a limited sustain capacity and short-term stability [22]. Additionally, the contrast between bright and dark zones reflects where the light was able to cross the gel structure, thus indicating that shadows represent the intense crosslinked polymeric network that is not crossed by light. On the other hand, the presence of bright areas may indicate the presence of pores and channels into the hydrogel network. The porosity and the pore magnitude, observed through the microscopic evaluation (**Error! Reference source not found.**), can exert direct influence in the water absorption profile, increasing the surface area which promotes capillary effect [47]. In this way, water, nutrients and even microorganisms, can be entrapped in the 3D network and be released from hydrogel in response to gradient condition changes.

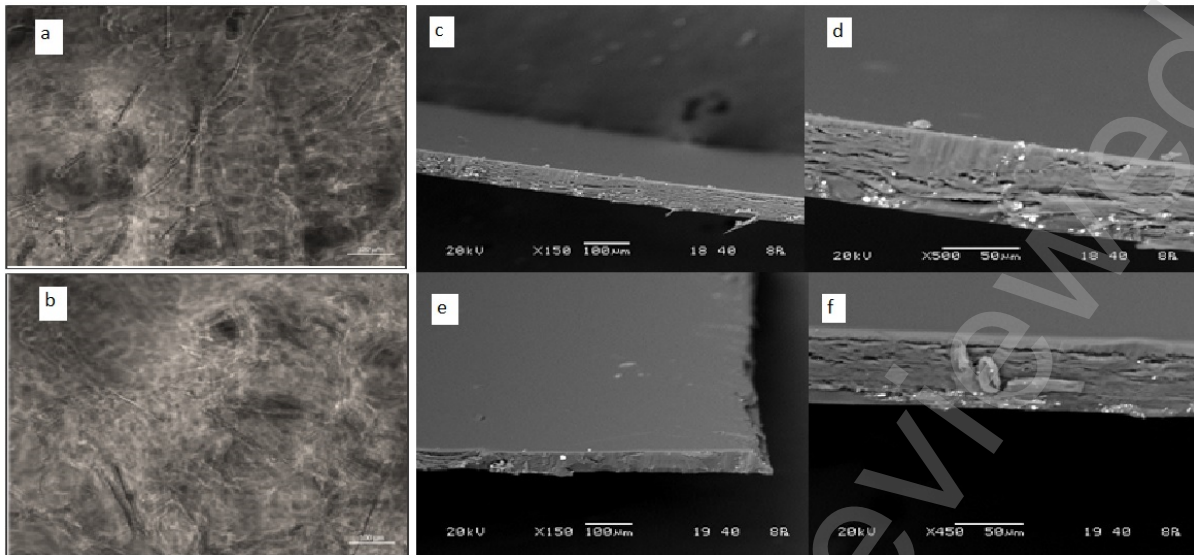


Figure 2. Optical microscopy of cellulose based hydrogels prototypes a) H1 and b) H2. Scanning electronic microscopy of cellulose hydrogel prototypes crosslinked with epichlorohydrin at x150 and at x 450-500 magnification c) and d) for H1, respectively and e) and f) for H2 respectively. Note: H1 – cellulose-based hydrogel synthesized using natural cellulose fibers extracted from sugarcane bagasse; H2 – cellulose-based hydrogel synthesized using commercial cellulose from Sigma-Aldrich.

Structural morphology of both hydrogels was investigated *via* SEM, enabling the visualization of smooth and homogeneous surface, with the presence of multilayers in the transversal cutting in both dried hydrogels, after drying process (**Error! Reference source not found.**). The use of cellulose materials obtained from sugarcane bagasse showed similar morphology in the organization of 3D structure compared to the hydrogels manufactured from commercial cellulose from Sigma-Aldrich.

### FT-IR spectroscopy

FT-IR was performed to characterize and identify the main functional groups of both cellulose materials used in the development of hydrogels, before and after the chemical crosslinking with epichlorohydrin. Both hydrogels presented very similar FT-IR spectrum as shown in **Error! Reference source not found.** It was possible to observe a similar band at  $3356\text{ cm}^{-1}$ , assigned to OH stretching vibration, and at  $2924\text{ cm}^{-1}$  attributed to the CH stretching of the polymer [47]. Around  $1593\text{ cm}^{-1}$ , a vibration band is observed related to carbonyl stretching of  $-\text{COO}-$  group, which is characteristic of CMC [47,48]. Additionally, the absorption band at  $1347\text{ cm}^{-1}$  reflects the  $\text{CH}_2$  bending of scissoring type, which is reported in the CMC spectrum [48].



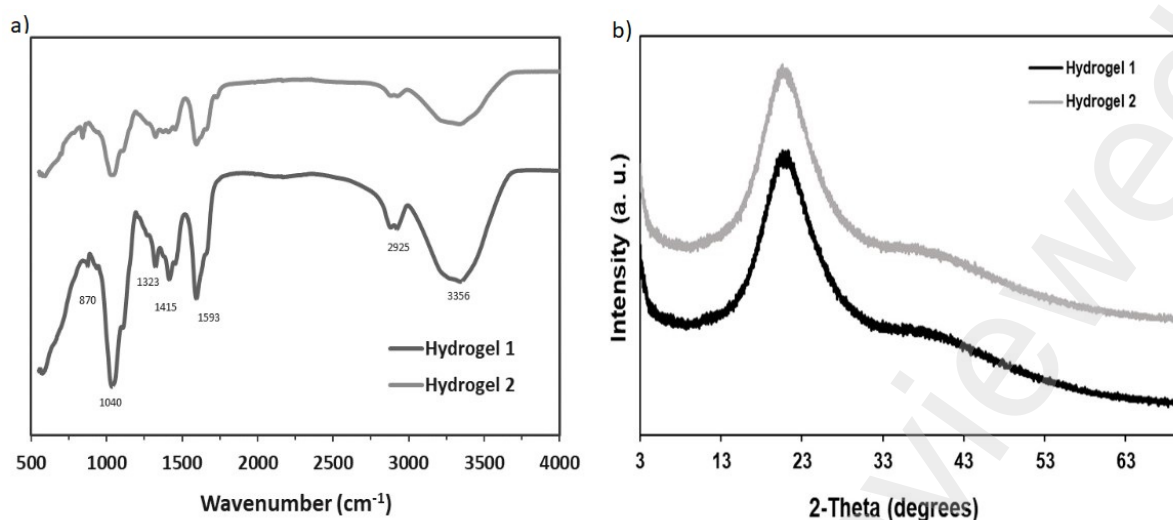


Figure 3. a) FTIR spectra of cellulose-based hydrogel prototype 1 (H1) and 2 (H2). b) Powder X-Ray diffraction patterns of hydrogel prototypes H1 and H2. Note: H1 – cellulose-based hydrogel synthesized using natural cellulose fibers extracted from sugarcane bagasse; H2 cellulose-based hydrogel synthesized using commercial cellulose from Sigma-Aldrich.

The chemical crosslinking between epichlorohydrin and hydroxyl groups of cellulose resulted in ether-based linkage. This type of functional group (C-O vibration) appeared as a band in  $1328\text{ cm}^{-1}$  in both hydrogels, indicating the effectiveness of crosslinking reaction [49]. In addition, a decrease in the band intensity at  $1430\text{ cm}^{-1}$ , known as crystallinity region, can be verified in both hydrogels, thus suggesting an increased capacity to absorb water [49].

### PXRD

The cellulose extracted from sugarcane bagasse, used in the development of hydrogel H1, presented a predominant crystalline type cellulose I, which is the most abundant type found in nature [50]. In the cellulose mercerization (under alkaline conditions) or in the regeneration process (dissolution and recrystallization), a shift from type I to type II occurs, resulting in a decrease of cellulose crystallinity. In the present work, both dried hydrogels showed a PXRD pattern similar to crystalline structure of cellulose II (**Error! Reference source not found.**). The diffraction peak appeared at  $2\theta$   $20.9^\circ$  and  $39.9^\circ$  for H1 and at  $2\theta$  was  $21.3^\circ$  and  $39.7^\circ$  for H2, with crystallinity index of  $27.3\% \pm 0.6$  and  $28.3\% \pm 0.7$  for H1 and H2, respectively. These results indicate that cellulose fibers in hydrogels possess crystalline and amorphous domains [46]. The crystalline regions of cellulose hydrogels have a more ordered and tightly packed arrangement of polymeric chains, providing structural integrity and mechanical strength of

the hydrogel. On the other hand, the amorphous domains are randomly oriented and have less ordered molecular arrangements, given to hydrogel matrices more accessible spaces and free volume for water molecules to penetrate and interact with, leading to an increased water absorption capacity [48].

## Thermal properties

### Differential Scanning Calorimetry

Differential scanning calorimetry (DSC) and thermogravimetry (TG) were performed in order to provide complementary information about the thermal events and stability of cellulose-based hydrogels. The results are summarized in Table 2 and Fig. S1 (Supplementary Materials).

Table 2. Thermal profile of hydrogels H1 and H2 determined by Differential Scanning Calorimetry (DSC) and Thermogravimetric analysis (TG).

Hydrogels	TG			DSC	
	Water Loss	Decomposition		Water Loss	Decomposition
H1	100.0 °C/9.9 %	160.0 °C/8.8 %	299.4 °C/45.3 %	77.8 °C	318.0 °C
H2	56.0 °C/11.4 %	---	290.6 °C/50.3 %	67.9 °C	310.0 °C

Note: H1 – cellulose-based hydrogel synthesized using natural cellulose fibers extracted from sugarcane bagasse; H2 cellulose-based hydrogel synthesized using commercial cellulose from Sigma-Aldrich.

Differential scanning calorimetry analysis was performed to understand the thermal behavior of hydrogel formulations. Fig. S1 illustrates two endothermic events, the first at 77.8 °C for prototype 1 (H1) and at 67.9 °C for prototype 2 (H2), which corresponds to the desorption of moisture in the polysaccharide structure [48]. For both samples, it was recorded a considerable shift for higher temperatures for prototype H1, with the highest enthalpy (i.e., 194.6 J g<sup>-1</sup>). This is likely due to a higher content of intrinsic bonded water which may be related to the lower size of cellulose particles composing these hydrogels or to the lower purity of cellulose fraction obtained from bagasse, in comparison to the cellulose from Sigma, which may contribute to retain water. This first event is followed by a second endothermic peak at ca. 220 and 218 °C for prototype 1 and 2, respectively. This secondary endothermic peak was attributed to the disintegration of glycosidic linkages and cellulose

depolymerization. After the two endothermic events, it was possible to observe an exothermic transition at ca. 318 °C for H1 and at 310 °C for H2, which is attributed to decomposition cellulose, suggesting that the prototype H1 may be more stable than the prototype H2 [48].

The thermal behavior of the cellulose-based hydrogels was also evaluated by means of TG analysis response and their corresponding first derivative curves. Thermogravimetric analysis of the H1 presented the peak of the first weight loss around 100 °C (9.9 %), which corresponds to the presence of water molecules, and the second weight loss event with a peak at 160 °C (8.8 %). Contrarily, the H2 presented the first weight loss event in a lower temperature (56 °C; 11.4 %), which indicates lower thermal stability of prototype 2, but on the other hand, it could facilitate the water release in drought conditions.

The H1 showed a significant weight loss at 299.4 °C (45.3 %) and H2 at 290.6 °C (50.6 %), which was attributed to the decomposition of CMC [49,51], i.e., loss of CO<sub>2</sub> from the polymeric backbone [48]. Cellulose-based hydrogels showed proper thermal stability and resistance to degradation, with superior stability exhibited by prototype 1 (H1), which can be explained by the difference in the pristine celluloses [49]. The chemical crosslinking performed seems to have generated strong intermolecular interaction within the cellulose network, thus providing structural integrity that prevents the hydrogel from collapsing or deforming at higher temperatures, making them promising prototypes for applications in arid and stressed environmental conditions.

### **Rheological evaluation**

The rheological evaluation of hydrogels, referring to storage and loss modulus ( $G'$  and  $G''$ , respectively) and viscosity (complex and instantaneous) are shown in **Error! Reference source not found.** The storage modulus ( $G'$ ) refers to the elasticity of the material, also denominated as dynamic rigidity, and reflects the reversible energy stored in the system [52]. Prototype H1 showed higher  $G'$  than H2 when submitted to increasing frequency. Thus, H1 presented higher elasticity than the hydrogel formulated with commercial cellulose from Sigma-Aldrich. Generally, the addition of fibers in hydrogels can have the purpose of improving the mechanical characteristics [53]. Therefore, the addition of

cellulose extracted from bagasse fulfilled the objective, promoting a positive impact on the mechanical properties of the hydrogel.

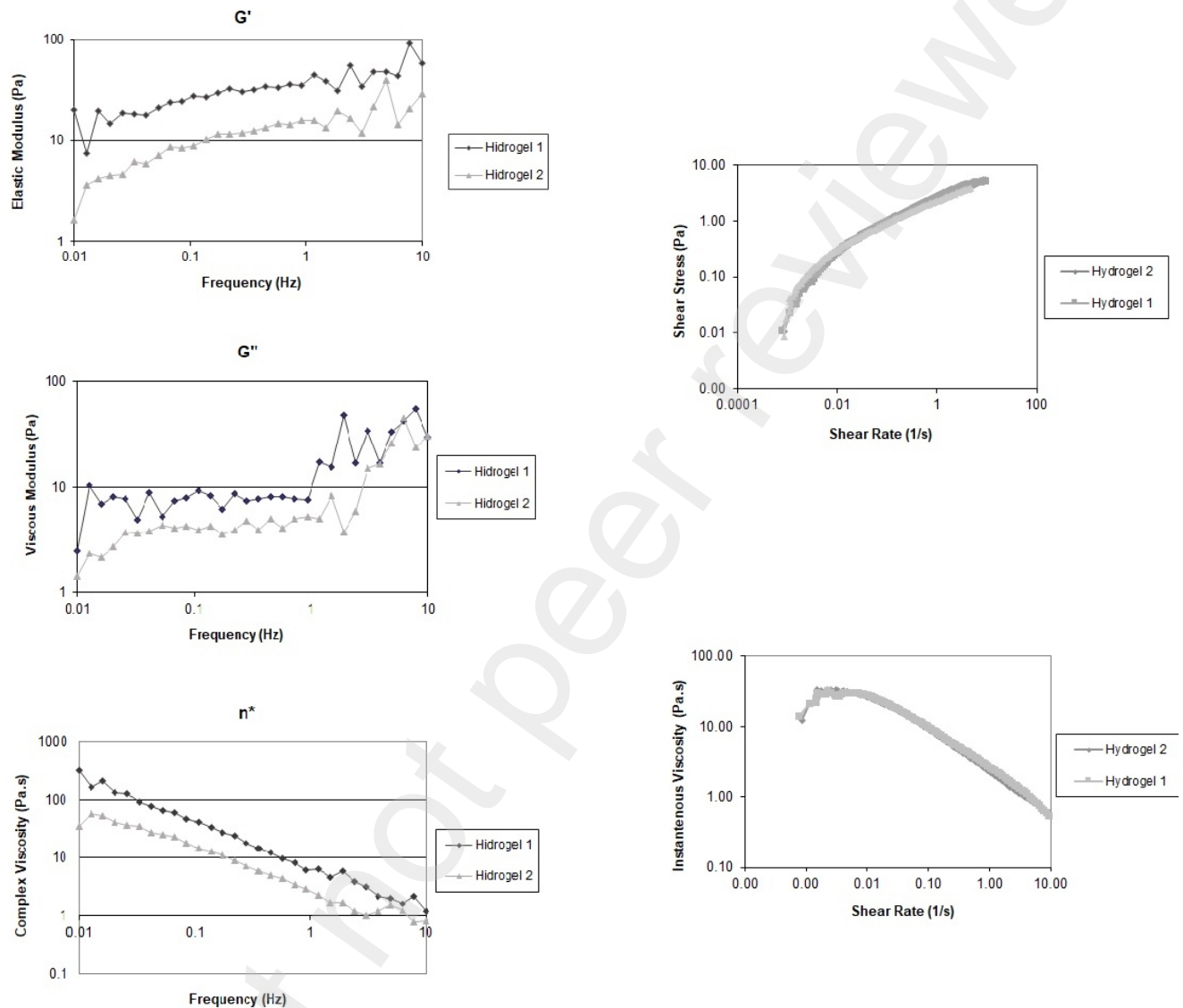


Figure 4. Rheological behavior of cellulose-based hydrogels H1 and H2. Note: H1 – cellulose-based hydrogel synthesized using natural cellulose fibers extracted from sugarcane bagasse; H2 cellulose-based hydrogel synthesized using commercial cellulose from Sigma-Aldrich.

The  $G''$  modulus is a measure of the viscosity of a solid-like material, which means that a viscous solid material will not change readily its form when submitted to shear. The prototype H1 showed higher  $G''$  than H2, regardless of the frequency applied. This is most likely to the addition of cellulose pulp, which presents more fibers in the structure of cellulose.

Regarding the steady-state viscosity versus shear rate, both hydrogels showed a similar Non-Newtonian behavior profile, with the decrease in viscosity as the shear rates increased. A similar behavior was also reported for acrylamide hydrogel reinforced with silica [54]. The proof that both hydrogels present a true gel-like structure was evident by the decrease of the complex viscosity as function of frequency (**Error! Reference source not found.**), since the Cox-Merz theoretical rule indicates that in the structure of the gels, the response of improving the frequency is the decreasing of complex viscosity [52].

### Texturometric Evaluation

The gel strength was measured as the force in compression, using a cylinder probe that penetrates 5 mm into the swollen hydrogel. The prototype H1 exhibited slightly superior gel strength ( $7.8 \pm 0.3$  g) than H2 ( $7.4 \pm 0.4$  g). The results of gel strength were in accordance with the rheological evaluation, showing that the addition of cellulose fibers from the sugarcane bagasse improves the overall mechanical properties of cellulose hydrogel crosslinked with epichlorohydrin. Additionally, this result reinforces that these prototypes could keep the structural properties under stress and consequently favor their nutrient slow-release, and their long-term stability, thus reducing the necessity of often use (i.e. reapplication) [55].

### Swelling and water absorption capacity

The swelling and absorption profile of hydrogel plays an essential role for its efficient application in the agriculture field. Consequently, the determination of these characteristics is crucial to understand the potential of these prototypes. All the results obtained for swelling capacity, including water and urea solution absorption, are shown in **Error! Reference source not found.**

Hydrogel H1 showed a water absorption capacity of ca. 160 g of water per  $g^{-1}$  of dried hydrogel over 1 h of contact, whereas H2 reached ca. 160 g of water per  $g^{-1}$  of dried hydrogel in the same period. These rapid water absorption rates suggest that these hydrogels can be used to absorb rapidly the water from occasional rain.

Table 3. Hydrogel swelling capacity by time of exposure in deionized water, type of salt, and urea concentration.

Hydrogel prototype	Deionized H <sub>2</sub> O (w/v)	Salt solutions (w/w) of hydrated hydrogel/g of dried hydrogel)	Sandy Soil (% H <sub>2</sub> O)	Urea solution
--------------------	----------------------------------	--	---------------------------------	---------------

	1h	24h	48h	NaCl	KCl	Na <sub>2</sub> SO <sub>4</sub>		0.1% (w/v)
H1	160.9 ± 35.4	170.5 ± 29.3	220.0 ± 34.1	39.7 ± 5.3	36.7 ± 4.5	33.2 ± 7.6	153.3 ± 53.9	56.5 ± 2.3
H2	192.5 ± 6.4	195.1 ± 37.5	212.4 ± 12.8	53.3 ± 1.7	52.2 ± 2.4	46.7 ± 6.8	175.9 ± 35.8	67.6 ± 6.7

Note: H1 – cellulose-based hydrogel synthesized using natural cellulose fibers extracted from sugarcane bagasse; H2 cellulose-based hydrogel synthesized using commercial cellulose from Sigma-Aldrich.

After 48h of contact, the swelling capacity reached more than 200g of water per g<sup>-1</sup> for both dried hydrogels (i.e. 220 and 212 g of water per g<sup>-1</sup> for both dried H1 and H2, respectively), which enables the classification of both prototypes as superabsorbent hydrogels [56]. The hydrogels reached the water absorption saturation within 4-5 days, and after this period, both prototypes were able to hold the water without losing their form or leaking. The results obtained for both prototypes are in the line with the obtained with synthetic polymers and suggest that can be commercialize in semi-hydrated or hydrated form. In fact, Cheng et al. (2015) [57] and Nascimento et al. (2021) [10] reported that anionic cross-linked acrylamide and potassium acrylate copolymers can absorb ca. 260 to 400 g of water per gram of gel, respectively. Also, a commercial product available in the market, i.e., STOCKOSORB® 660 (Evonik®), is reported to absorb up to 400 g of water per gram of gel.

Concerning to the effect of ionic strength on the water absorption capacity of hydrogels, it has been reported that the water absorption/swelling rate is highly affected by the ionic strength of salt solution. This is due to the greater amount of positive charges from the ions present in the solution, affecting the absorption of water molecules by the hydrogel matrix, which is less available to interact with the water molecules, thus resulting in a poor swelling capacity in this environment [49]. In fact, the water absorption capacity of cellulose prototypes was impacted by the ionic strength caused by NaCl, KCl and Na<sub>2</sub>SO<sub>4</sub> solutions (0.1 M) in a similar way (Table 3). However, they were still able to absorb more than 40-50 times the weight of water per gram of dried hydrogels, which allows their use in soils with strong ionic profile. A similar cellulose hydrogel crosslinked with epichlorohydrin was synthesized by Navarra et al. (2015) [49], and the authors reported a swelling rate around 2500 % in the presence of Na<sub>2</sub>SO<sub>4</sub> solution (0.5 M), which is significantly inferior to the swelling rates obtained for H1 and H2 (i.e., 3300 and 4600 %, respectively, Table 3). Thus, the presence of ions in the solution reduces the swelling kinetics of both prototypes and the type of salt used did not significantly influence the absorption of water by the hydrogels.

Regarding the water absorption in sandy soil, this type of soil presents low natural capacity for water retention, which results in a negative impact on crop cultivation. These soils present naturally a great quantity and variety of ions, which influence the water absorption by hydrogels. The developed prototypes showed a water absorption improve of ca. 150 % and 200 % for soil containing the H1 and H2 respectively, compared to soil without any amendment (Table 3).

Superabsorbent hydrogels are classified as soil amendments as they absorb water and nutrients and facilitate their controlled release, a critical goal in the application of hydrogels in agriculture. In this context, urea is one of the most important fertilizers, mainly due to its high nitrogen content (up to 50 %) and low cost [58]. However, it is not recommended to apply urea directly to the soil due to nitrogen leaching, and ammonia volatilization [58,59]. Therefore, the development of eco-friendly hydrogels that could facilitate a controlled release of urea, represents an interesting approach for agriculture applications [59]. Regarding the loading of urea solution, both hydrogels' prototypes presented high loading capacity, even at the highest urea concentration tested (5 %, w v<sup>-1</sup>) (data not shown). The presence of higher urea concentration (5 %, w v<sup>-1</sup>) had a more pronounced effect on the H2 prototype, as its loading capacity was ca. 1100 %, in contrast with H1, which was by  $\approx$  510 %, in comparison with swollen hydrogels with pure water. The hydrogels, after urea solution loading, were able to keep the form and did not present leaking signals, showing the commercialization potential of hydrogels for urea-controlled release.

### **Hydrogels safety**

To evaluate the potential release of harmful compounds, e.g., derivatives of epichlorohydrin reaction with cellulose matrix, from the hydrogel prototypes, it was developed a degradation procedure using Celluclast commercial preparation to promote the degradation of both hydrogels. The Celluclast preparation is composed by a blend of cellulolytic enzymes from microbial fungi, and it was chosen due to its capacity to decompose lignocellulosic materials in nature [60]. This experiment was performed to mimic the natural degradation of this type of products (i.e., cellulose based-SAP hydrogels) in the soil environment to ensure the ecological safety of cellulose hydrogels. According to the results, no free residue of epichlorohydrin was released from the hydrogels H1 and H2, as can be seen in the

chromatograms in Fig. 2S. The other components used in the hydrogel's synthesis, such as cellulose and urea, are not a target of concern, since the polymer is biodegradable and is found in nature, and the nitrogen compound is already commercialized as a soil nutrient. Additionally, as mentioned before, the pH and conductivity values of the hydrogels showed a low probability of the presence of non-reactant compounds, since the pH is neutral, and the conductivity is below  $10.0 \mu\text{S cm}^{-1}$ . Therefore, regarding potentially hazardous chemical compounds released to the environment, the synthesized hydrogels can be considered safe.

In addition to this safety evaluation, the impact of adding the hydrogels to soil was also evaluated upon the microorganisms usually present there to assure the safety concerning soil microorganisms. Maintaining the natural microbiome is vital for promoting plant growth, efficient nutrient uptake, resistance to external factors, and other positive effects [44]. The results showed that hydrogels H1 and H2 did not negatively affect bacterial growth since no halos of inhibition were observed in MHA plates (Fig. S3). These findings suggest that the impact of hydrogels on soil microbial communities is likely to be minimal.

#### **Impact of urea-loaded hydrogels on maize seed germination**

Maize germination was inhibited when exposed to urea concentrations exceeding 2 %, and it was reduced at 1 % ( $\approx 10\text{-}40$  % of germination rate) and 0.5 % ( $\approx 80$  %). On the other hand, at a concentration of 0.1 % all maize seeds germinated (data not shown). As a result, this concentration was used to load hydrogels H1 and H2 to assess seedling growth and maize vigor index under their exposure. Results showed that H1 and H2 loaded with 0.1 % of urea significantly increased root length and vigor index (Table 4). These results underscore their safety for application during sowing and their ability to promote seedling development.

Table 4. Effect of hydrogels H1 and H2 loaded with 0.1 % urea on seedlings' root and shoot length, and Vigor index.

Treatment	Root length (mm)	Shoot length (mm)	Vigor index*
C	$75.50 \pm 0.59$ b	$41.78 \pm 3.40$ a	$11731 \pm 301$ b
H1	$88.78 \pm 6.74$ a	$42.83 \pm 3.66$ a	$13375 \pm 499$ a



H2	90.92 ± 1.35 a	49.67 ± 4.94 a	13845 ± 419 a
	**F=13.15	NS F=3.511	**F=21.56

Note: Results are expressed as mean ± SD. One-way ANOVA was performed to determine the influence of hydrogels on root and shoot seedlings' length and on vigor index. Means in the same column with different letters are significantly different from each other according to the Duncan test. The test results are shown with the test statistic and as NS non-significant  $p > 0.05$ , \*\* significant at  $p < 0.01$ ; \*\*\* significant at  $p < 0.001$ . \* Vigor index = (seedling root length + seedling shoot length) \* % germination rate. The germination rate was 100% in all treatments.

## Greenhouse pot experiment

### Shoot elongation and biomass

From the results presented in Figure 5 and Figure S4, it is possible to observe that shoot elongation generally decreased with reduced irrigation in the control pots. However, under 75 and 50 % irrigation, the use of hydrogels generally resulted in an enhanced shoot elongation (Figure 5a). In addition, the shoot elongation of plants grown with hydrogels under 75 % water irrigation was identical to those grown under full irrigation (Figure 5b). Both dry and fresh shoot biomass also showed a decline along the irrigation water gradient in the control pots (Figure 5b-d). Conversely, the use of hydrogels led to a significant increase in maize biomass. Although on fresh biomass this effect was more pronounced under 75 % irrigation, on dry biomass an increase was observed in all treatments regardless of the irrigation regime and surpassed the biomass of non-amended plants grown under full irrigation. Root biomass was also significantly increased by hydrogels irrespective of the irrigation regime (Figure 5d). At 75 % irrigation, treatments with H1 and H2 presented root biomasses approximately four times higher than in control pots and showed a higher positive effect than the commercial hydrogel (P).

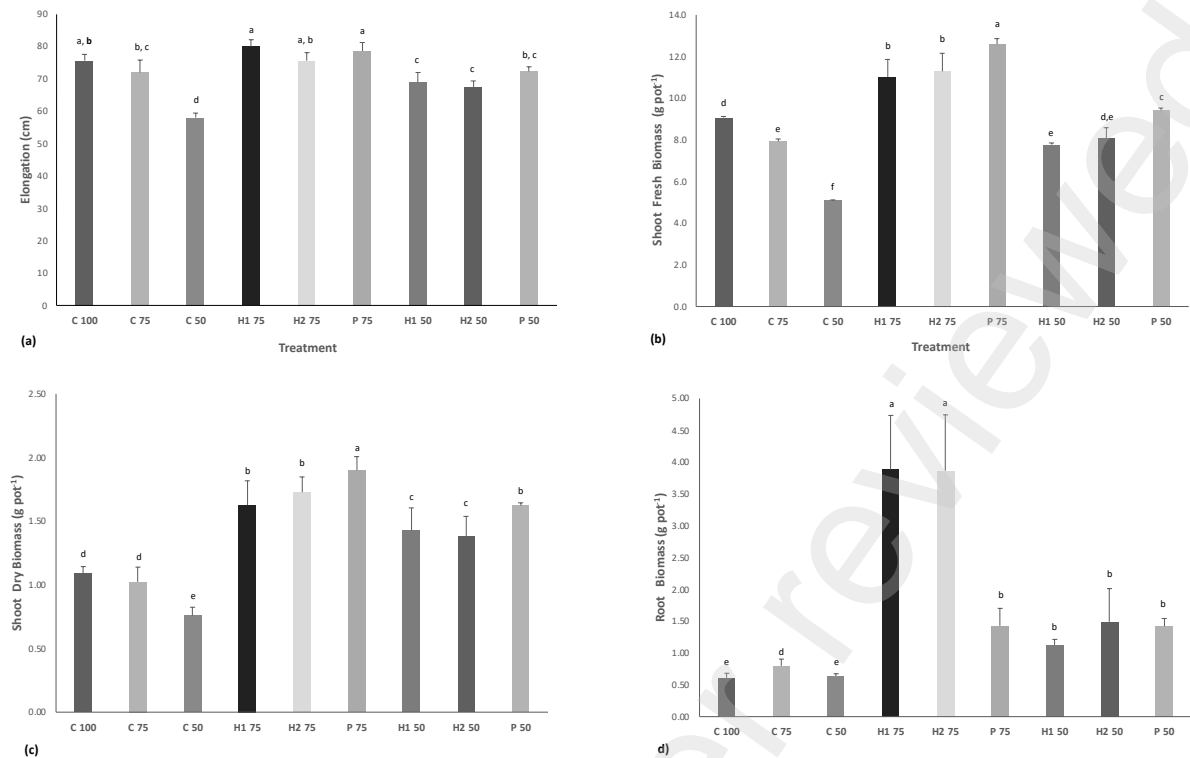


Figure 5. Shoot elongation (a), fresh biomass (b), and shoot (c) and root dry biomass (d) of maize plants grown in agricultural soil amended with a commercial hydrogel (P) and with hydrogels loaded with 0.1 % urea (H1 and H2) under different irrigation regimes (100 - full irrigation; 75 - irrigation at 75 % of maize needs; 50 - irrigation at 50 % of maize needs). The error bar represents the SD (n=5). Means for the different treatments with different letters are significantly different from each other ( $p < 0.05$ ) according to the Duncan test. For shoot fresh biomass and elongation, shoot and root dry biomass, the  $F$  values of one-way ANOVA, were respectively \*\*\*  $F=42.12$ , \*\*\* $F=39.79$ , \*\*\* $F=44.98$  and \*\*\* $F=63.74$ . The test results are shown with the test statistic and as \*\*\* significant at  $p < 0.001$ .

The increase in maize biomass in response to hydrogel treatments under water deficit could be attributed to their capacity to retain and release water when required by plants [61]. A significantly higher water retention in the plants treated with the hydrogels was observed, with control plants under full irrigation (C\_100) having lower water content than plants treated with hydrogels at 75 % water irrigation (data not shown;  $F=40.58$ ,  $p < 0.001$ ) (Fig. S4). This observation is supported by the soil moisture data from the control pots (Table 6). In the cases of both full and 75 % irrigation regimes, they demonstrated greater water retention in soil, compared to the hydrogel-treated pots, thereby highlighting the hydrogels' capacity to augment water absorption by plants.

The increase in maize biomass can also be attributed to the fertilizing role of the hydrogels (Fig. S5). The urea solution loaded in hydrogels H1 and H2 was likely released from their structure to the soil matrix [62] and converted into readily assimilable N forms, such as

ammonium (NH<sub>4</sub><sup>+</sup>) [63]. This was also reflected in the heightened physiological nitrogen use (pNUE<sub>N</sub>) among plants grown with the hydrogel (Table 5). The increase in the pNUE<sub>N</sub> was particularly noteworthy in plants treated with H1 and H2 at 75 % irrigation, as well as under H2 treatment at 50 % irrigation. Nitrogen is recognized as one of the essential nutrients for plant growth, playing a critical role in many biological processes, including stress resilience [64].

Hydrogels also exhibit the potential to serve as a reservoir for soil nutrients, including phosphorous (P) and potassium (K), facilitating their uptake by plants. In fact, the pNUEs of these elements were also increased in plants under hydrogels treatments, following the trend observed for N, irrespective of the irrigation system (Table 5). The results are therefore in accordance with the often-reported positive impacts of hydrogels on plant growth promotion under water stress conditions [65–67].

Table 5. Physiological nutrient (N, P and K) use efficiency (pNUE) of maize plants grown in agricultural soil amended with a commercial hydrogel (P), and with hydrogels loaded with 0.1 % urea (H1 and H2) under different irrigation regimes (100 - full irrigation; 75 - irrigation at 75 % of maize needs; 50 - irrigation at 50 % of maize needs).

Treatment	pNUE <sub>N</sub>	pNUE <sub>P</sub>	pNUE <sub>K</sub>
C 100	124.76 ± 7.92 <sup>c</sup>	141.51 ± 3.31 <sup>e</sup>	40.25 ± 2.56 <sup>d</sup>
C 75	130.70 ± 3.47 <sup>c</sup>	139.1 ± 2.66 <sup>e</sup>	42.14 ± 4.02 <sup>d</sup>
H1 75	275.03 ± 73.54 <sup>a</sup>	294.47 ± 23.24 <sup>a</sup>	119.58 ± 16.83 <sup>a</sup>
H2 75	208.26 ± 38.25 <sup>b</sup>	266.26 ± 30.57 <sup>b</sup>	119.00 ± 38.34 <sup>a</sup>
P 75	153.23 ± 49.64 <sup>bc</sup>	213.60 ± 18.74 <sup>cd</sup>	55.94 ± 11.29 <sup>cd</sup>
C 50	116.41 ± 6.29 <sup>c</sup>	147.29 ± 10.55 <sup>e</sup>	47.76 ± 3 <sup>d</sup>
H1 50	123.02 ± 4.89 <sup>c</sup>	193.15 ± 7.87 <sup>d</sup>	73.04 ± 3.55 <sup>bc</sup>
H2 50	169.26 ± 77.68 <sup>bc</sup>	220.08 ± 34.81 <sup>cd</sup>	81.6 ± 12.79 <sup>b</sup>
P 50	133.77 ± 50.1 <sup>c</sup>	224.31 ± 16.83 <sup>c</sup>	61.25 ± 10.13 <sup>bcd</sup>
	*** F=5.999	*** F=34.42	*** F=16.95

Note: Means in the same column with different letters are significantly different from each other according to the Duncan test. The test results are shown with the test statistic and as \*\*\* significant at p<0.001.

Soil pH and EC are important factors in soil chemical and biological properties. The use of urea can lead to a reduction in soil pH due to the release of ammonium (NH<sub>4</sub><sup>+</sup>) [68], but despite its use in H1 and H2, no significant changes in soil pH were observed across the treatments (Table 6). Conversely, a significantly higher EC was detected in soils containing the commercial hydrogel (P50 and P75). Shahid et al. (2012) [69] and Pavarthi et al. (2014) [70] reported an increase in soil EC upon the application of synthetic hydrogels, which was attributed to the contained ions. The EC was also significantly higher in C50 than in the other treatments,

indicative of a higher concentration of elements in the soil likely due to the lower moisture levels (Table 6). In fact, EC was negatively correlated (data not shown) with soil moisture.

Table 6. Soil moisture, pH and EC at the end of the greenhouse pot experiment

Treatment	Moisture	pH	EC
C 100	30 ± 3.7 <sup>a</sup>	6.8 ± 0.1 <sup>a</sup>	288.2 ± 5.6 <sup>e</sup>
C 75	11.6 ± 1.2 <sup>b</sup>	6.8 ± 0.1 <sup>a</sup>	299.8 ± 12.6 <sup>de</sup>
C 50	6 ± 0.3 <sup>de</sup>	6.7 ± 0.1 <sup>a</sup>	324.2 ± 19.4 <sup>bc</sup>
H1 75	8.5 ± 1 <sup>c</sup>	6.8 ± 0.1 <sup>a</sup>	290.4 ± 11 <sup>e</sup>
H2 75	7.9 ± 0.5 <sup>c</sup>	6.8 ± 0.1 <sup>a</sup>	285 ± 7.8 <sup>e</sup>
P 75	7.2 ± 1.2 <sup>cd</sup>	6.5 ± 0.1 <sup>a</sup>	328.2 ± 6.3 <sup>b</sup>
H1 50	5.4 ± 0.7 <sup>e</sup>	6.7 ± 0.1 <sup>a</sup>	309.2 ± 6.5 <sup>cd</sup>
H2 50	6.2 ± 0.3 <sup>de</sup>	6.7 ± 0.1 <sup>a</sup>	288 ± 5.9 <sup>e</sup>
P 50	5.3 ± 0.5 <sup>e</sup>	6.6 ± 0.1 <sup>a</sup>	359.4 ± 19.1 <sup>a</sup>
	***F=111.2	NS	***F=22.86

Means in the same column with different letters are significantly different from each other ( $p < 0.05$ ) according to the Duncan test. The test results are shown with the test statistic and as *NS* non-significant at  $p > 0.05$ , and \*\*\* significant at  $p < 0.001$ .

#### 4. Conclusion

The results demonstrate that the sugarcane-based hydrogels exhibit promising characteristics for use as soil amendment or as biofertilizers. They present high water swelling capacity, resistance to high osmotic pressure solutions and great urea absorption capabilities. These hydrogels were able to load up to 67 times their own weight of urea solution, underscoring their potential to be used as superabsorbent amendments. Additionally, the eco-friendly approach used in the synthesis process, which excludes acrylates and acrylamide from the composition, allows our hydrogels to be an interesting and more sustainable alternative for agricultural applications. This was also supported by the greenhouse pot experiment, where the plants grown with H1 and H2 (loaded with 0.1 % of urea solution), under two levels of irrigation (75 and 50 % of irrigation), showed a similar development when compared to those grown with the commercial hydrogel. It is crucial to highlight that our hydrogels were developed mainly with bio-based raw materials, without epichlorohydrin in the leaching liquid, and with no impact on soil bacteria, which strongly indicates the environmental safety of our products. Regarding production costs, H1 probably is a more economically feasible

option since it is made with carboxymethyl cellulose and cellulose extracted from sugarcane

## Acknowledgements

Authors would like to thank to Raízen for the kindly supply of bagasse feedstock. Project co-financed by the European Regional Development Fund (ERDF), through the Operational Program for Competitiveness and Internationalization (COMPETE 2020) and Portugal 2020, under the Alchemy Project (POCI-01-0247-FEDER-027578). We would also like to thank the scientific collaboration under the FCT project UID/Multi/50016/2020.

## REFERENCES

- [1] M.A. Caretta, A. Mukherji, M. Arfanuzzaman, R.A. Betts, A. Gelfan, Y. Hirabayashi, T.K. Lissner, J. Liu, E. Lopez Gunn, R. Morgan, S. Mwanga, S. Supratid, Water. In: *Climate Change 2022: Impacts, Adaptation, and Vulnerability. Contribution of Working Group II to the Sixth Assessment Report of the Intergovernmental Panel on Climate Change* [H.-O. Pörtner, D.C. Roberts, M. Tignor, E.S. Poloczanska, K. Mintenbeck, A. Alegría, M. Craig, S. Langsdorf, S. Löschke, V. Möller, A. Okem, B. Rama (eds.)], in: Cambridge University Press. In Press., 2022.
- [2] World Health Organization, Drought, (2023). [https://www.who.int/health-topics/drought#tab=tab\\_1](https://www.who.int/health-topics/drought#tab=tab_1) (accessed August 30, 2023).
- [3] I.R. Orimoloye, J.A. Belle, Y.M. Orimoloye, A.O. Olusola, O.O. Ololade, Drought: A Common Environmental Disaster, *Atmosphere (Basel)*. 13 (2022). <https://doi.org/10.3390/atmos13010111>.
- [4] FAO, The impact of disasters and crises on agriculture and food security: 2021, FAO, 2021. <https://doi.org/10.4060/cb3673en>.
- [5] S. Malik, K. Chaudhary, A. Malik, H. Punia, M. Sewhag, N. Berkesia, M. Nagora, S. Kalia, K. Malik, D. Kumar, P. Kumar, E. Kamboj, V. Ahlawat, A. Kumar, K. Boora, Superabsorbent Polymers as a Soil Amendment for Increasing Agriculture Production with Reducing Water Losses under Water Stress Condition, *Polymers (Basel)*. 15 (2023). <https://doi.org/10.3390/polym15010161>.
- [6] N. Mazloom, R. Khorassani, G.H. Zohury, H. Emami, J. Whalen, Lignin-based hydrogel alleviates drought stress in maize, *Environ Exp Bot*. 175 (2020). <https://doi.org/10.1016/j.envexpbot.2020.104055>.
- [7] United Nations, The Drought Initiative , (n.d.). <https://www.unccd.int/land-and-life/drought/drought-initiative> (accessed August 30, 2023).
- [8] S. Malik, K. Chaudhary, A. Malik, H. Punia, M. Sewhag, N. Berkesia, M. Nagora, S. Kalia, K. Malik, D. Kumar, P. Kumar, E. Kamboj, V. Ahlawat, A. Kumar, K. Boora, Superabsorbent Polymers as a Soil Amendment for Increasing Agriculture Production with Reducing Water Losses under Water Stress Condition, *Polymers (Basel)*. 15 (2023). <https://doi.org/10.3390/polym15010161>.

- [9] H. Zheng, P. Mei, W. Wang, Y. Yin, H. Li, M. Zheng, X. Ou, Z. Cui, Effects of super absorbent polymer on crop yield, water productivity and soil properties: A global meta-analysis, *Agric Water Manag.* 282 (2023). <https://doi.org/10.1016/j.agwat.2023.108290>.
- [10] C.D.V. Nascimento, R.W. Simmons, J.P. de A. Feitosa, C.T. dos S. Dias, M.C.G. Costa, Potential of superabsorbent hydrogels to improve agriculture under abiotic stresses, *J Arid Environ.* 189 (2021). <https://doi.org/10.1016/j.jaridenv.2021.104496>.
- [11] Khushbu, S.G. Warkar, A. Kumar, Synthesis and assessment of carboxymethyl tamarind kernel gum based novel superabsorbent hydrogels for agricultural applications, *Polymer (Guildf)*. 182 (2019). <https://doi.org/10.1016/j.polymer.2019.121823>.
- [12] H. Zheng, P. Mei, W. Wang, Y. Yin, H. Li, M. Zheng, X. Ou, Z. Cui, Effects of super absorbent polymer on crop yield, water productivity and soil properties: A global meta-analysis, *Agric Water Manag.* 282 (2023). <https://doi.org/10.1016/j.agwat.2023.108290>.
- [13] G.H.A. El-Aziz, A.S. Ibrahim, A.H. Fahmy, Using Environmentally Friendly Hydrogels to Alleviate the Negative Impact of Drought on Plant, *Open Journal of Applied Sciences.* 12 (2022) 111–133. <https://doi.org/10.4236/ojapps.2022.121009>.
- [14] L. Chang, L. Xu, Y. Liu, D. Qiu, Superabsorbent polymers used for agricultural water retention, *Polym Test.* 94 (2021). <https://doi.org/10.1016/j.polymertesting.2020.107021>.
- [15] M. Shahzamani, S. Taheri, A. Roghanizad, N. Naseri, M. Dinari, Preparation and characterization of hydrogel nanocomposite based on nanocellulose and acrylic acid in the presence of urea, *Int J Biol Macromol.* 147 (2020) 187–193. <https://doi.org/10.1016/j.ijbiomac.2020.01.038>.
- [16] B. Grabowska-Polanowska, T. Garbowski, D. Bar-Michalczyk, A. Kowalczyk, The benefits of synthetic or natural hydrogels application in agriculture: An overview article, *Journal of Water and Land Development.* 51 (2021) 208–224. <https://doi.org/10.24425/jwld.2021.139032>.
- [17] A. Sikder, A.K. Pearce, S.J. Parkinson, R. Napier, R.K. O'Reilly, Recent Trends in Advanced Polymer Materials in Agriculture Related Applications, *ACS Appl Polym Mater.* 3 (2021) 1203–1217. <https://doi.org/10.1021/acsapm.0c00982>.
- [18] S. Li, G. Chen, Agricultural waste-derived superabsorbent hydrogels: Preparation, performance, and socioeconomic impacts, *J Clean Prod.* 251 (2020). <https://doi.org/10.1016/j.jclepro.2019.119669>.
- [19] J. Ma, X. Li, Y. Bao, Advances in cellulose-based superabsorbent hydrogels, *RSC Adv.* 5 (2015) 59745–59757. <https://doi.org/10.1039/c5ra08522e>.
- [20] Y. Liu, J. Wang, H. Chen, D. Cheng, Environmentally friendly hydrogel: A review of classification, preparation and application in agriculture, *Science of the Total Environment.* 846 (2022). <https://doi.org/10.1016/j.scitotenv.2022.157303>.
- [21] N. Serrano-Silva, M. Luna-Guido, F. Fernández-Luqueño, R. Marsch, L. Dendooven, Emission of greenhouse gases from an agricultural soil amended with urea: A laboratory study, *Applied Soil Ecology.* 47 (2011) 92–97. <https://doi.org/10.1016/j.apsoil.2010.11.012>.
- [22] S.D. Palanivelu, N.A.Z. Armir, A. Zulkifli, A.H.A. Hair, K.M. Salleh, K. Lindsey, M.H. Che-Othman, S. Zakaria, Hydrogel Application in Urban Farming: Potentials and Limitations—A Review, *Polymers (Basel).* 14 (2022). <https://doi.org/10.3390/polym14132590>.

- [23] L. Zhang, Y. Guan, Microbial investigations of new hydrogel-biochar composites as soil amendments for simultaneous nitrogen-use improvement and heavy metal immobilization, *J Hazard Mater.* 424 (2022). <https://doi.org/10.1016/j.jhazmat.2021.127154>.
- [24] H. Wang, W. Bai, X. Peng, W. Han, J. He, J. Song, G. Lv, Effect of super absorbent polymer sodium polyacrylate on the bacterial community and associated chemistry of loessial soil, *Arch Agron Soil Sci.* 66 (2020) 70–82. <https://doi.org/10.1080/03650340.2019.1597268>.
- [25] A.A. Albalasmeh, O. Mohawesh, M.A. Gharaibeh, A.G. Alghamdi, M.A. Alajlouni, A.M. Alqudah, Effect of hydrogel on corn growth, water use efficiency, and soil properties in a semi-arid region, *Journal of the Saudi Society of Agricultural Sciences.* 21 (2022) 518–524. <https://doi.org/10.1016/j.jssas.2022.03.001>.
- [26] A. Sannino, M. Madaghiele, F. Conversano, G. Mele, A. Maffezzoli, P.A. Netti, L. Ambrosio, L. Nicolais, Cellulose derivative-hyaluronic acid-based microporous hydrogels cross-linked through divinyl sulfone (DVS) to modulate equilibrium sorption capacity and network stability, *Biomacromolecules.* 5 (2004) 92–96. <https://doi.org/10.1021/bm0341881>.
- [27] H. Kono, Characterization and properties of carboxymethyl cellulose hydrogels crosslinked by polyethylene glycol, *Carbohydr Polym.* 106 (2014) 84–93. <https://doi.org/10.1016/j.carbpol.2014.02.020>.
- [28] S. Khairunnisa, I. Rostini, The effect of glycerol concentration as a plasticizer on edible films made from alginate towards its physical characteristic, 2018. [www.worldscientificnews.com](http://www.worldscientificnews.com).
- [29] EN 1097-6:2022, EN 1097-6:2022. Tests for mechanical and physical properties of aggregates - Part 6: Determination of particle density and water absorption, EN 1097-6: 2022. (2022).
- [30] V. Dhanapal, P. Subhapriya, K.P. Nithyanandam, M. V. Kiruthika, T. Keerthana, G. Dineshkumar, Design, synthesis and evaluation of N,N1-methylenebisacrylamide crosslinked smart polymer hydrogel for the controlled release of water and plant nutrients in agriculture field, in: *Mater Today Proc*, Elsevier Ltd, 2021: pp. 2491–2497. <https://doi.org/10.1016/j.matpr.2020.11.101>.
- [31] M. Cai, Y. Zou, Trace Level Analysis of Epichlorohydrin in Drinking Water by Gas Chromatography/ Flame Ionization Detector, 2010.
- [32] O. Tarawneh, H. Abu Mahfouz, L. Hamadneh, A.A. Deeb, I. Al-Sheikh, W. Alwahsh, A. Fadhil Abed, Assessment of persistent antimicrobial and anti-biofilm activity of p-HEMA hydrogel loaded with rifampicin and cefixime, *Sci Rep.* 12 (2022). <https://doi.org/10.1038/s41598-022-07953-3>.
- [33] J. Hudzicki, Kirby-Bauer Disk Diffusion Susceptibility Test Protocol, 2009. [www.atcc.org](http://www.atcc.org).
- [34] M.O.G. Ferreira, L.L.R. Leite, I.S. de Lima, H.M. Barreto, L.C.C. Nunes, A.B. Ribeiro, J.A. Osajima, E.C. da Silva Filho, Chitosan Hydrogel in combination with Nerolidol for healing wounds, *Carbohydr Polym.* 152 (2016) 409–418. <https://doi.org/10.1016/j.carbpol.2016.07.037>.
- [35] M. Balouiri, M. Sadiki, S.K. Ibnsouda, Methods for in vitro evaluating antimicrobial activity: A review, *J Pharm Anal.* 6 (2016) 71–79. <https://doi.org/10.1016/j.jpha.2015.11.005>.

- [36] S.I.A. Pereira, P.M.L. Castro, Phosphate-solubilizing rhizobacteria enhance Zea mays growth in agricultural P-deficient soils, *Ecol Eng.* 73 (2014) 526–535. <https://doi.org/10.1016/j.ecoleng.2014.09.060>.
- [37] S.I.A. Pereira, P.M.L. Castro, Phosphate-solubilizing rhizobacteria enhance Zea mays growth in agricultural P-deficient soils, *Ecol Eng.* 73 (2014) 526–535. <https://doi.org/10.1016/j.ecoleng.2014.09.060>.
- [38] C.S.C. Calheiros, S.I.A. Pereira, P.M.L. Castro, Culturable bacteria associated to the rhizosphere and tissues of *Iris pseudacorus* plants growing in a treatment wetland for winery wastewater discharge, *Ecol Eng.* 115 (2018) 67–74. <https://doi.org/10.1016/j.ecoleng.2018.02.011>.
- [39] H.T.T. Nguyen, C. Van Pham, P. Bertin, The effect of nitrogen concentration on nitrogen use efficiency and related parameters in cultivated rices (*Oryza sativa* L. subsp. *indica* and *japonica* and *O. glaberrima* Steud.) in hydroponics, *Euphytica.* 198 (2014) 137–151. <https://doi.org/10.1007/s10681-014-1101-9>.
- [40] V.J.G. Houba, J.J. Van der Lee, I. Novozamsky, Soil Analysis Procedures, in: Department of Soil Science and Plant Nutrition, Wageningen Agricultural University, Syllabus, Wageningen., Wageningen, 1995.
- [41] R. Freixo, F. Casanova, A.B. Ribeiro, C.F. Pereira, E.M. Costa, M.E. Pintado, Ó.L. Ramos, Extraction methods and characterization of cellulose fractions from a sugarcane by-product for potential industry applications, *Ind Crops Prod.* 197 (2023). <https://doi.org/10.1016/j.indcrop.2023.116615>.
- [42] T. Liebert, Cellulose Solvents – Remarkable History, Bright Future, in: Cellulose Solvents: For Analysis, Shaping and Chemical Modification, ACS Symposium Series; American Chemical Society, Washington, DC, 2010: pp. 1–54.
- [43] B. Medronho, A. Romano, M.G. Miguel, L. Stigsson, B. Lindman, Rationalizing cellulose (in)solubility: Reviewing basic physicochemical aspects and role of hydrophobic interactions, *Cellulose.* 19 (2012) 581–587. <https://doi.org/10.1007/s10570-011-9644-6>.
- [44] J.M. Chaparro, A.M. Sheflin, D.K. Manter, J.M. Vivanco, Manipulating the soil microbiome to increase soil health and plant fertility, *Biol Fertil Soils.* 48 (2012) 489–499. <https://doi.org/10.1007/s00374-012-0691-4>.
- [45] O. Ajao, J. Jeaidi, M. Benali, A.M. Restrepo, N. El Mehdi, Y. Boumghar, Quantification and variability analysis of lignin optical properties for colour-dependent industrial applications, *Molecules.* 23 (2018). <https://doi.org/10.3390/molecules23020377>.
- [46] K. Nakasone, T. Kobayashi, Cytocompatible cellulose hydrogels containing trace lignin, *Materials Science and Engineering C.* 64 (2016) 269–277. <https://doi.org/10.1016/j.msec.2016.03.108>.
- [47] A. Hebeish, M. Elrafie, A. Rabie, A. Aly, D. Refaat, Synthesis and Properties of Superabsorbent Carboxymethyl Cellulose Graft-Poly(acrylic acid-co-acrylamide), 2015.
- [48] N.A. Dahlan, J. Pushpamalar, A.K. Veeramachineni, S. Muniyandy, Smart Hydrogel of Carboxymethyl Cellulose Grafted Carboxymethyl Polyvinyl Alcohol and Properties Studied for



- Future Material Applications, *J Polym Environ.* 26 (2018) 2061–2071.  
<https://doi.org/10.1007/s10924-017-1105-3>.
- [49] M.A. Navarra, C. Dal Bosco, J.S. Moreno, F.M. Vitucci, A. Paolone, S. Panero, Synthesis and characterization of cellulose-based hydrogels to be used as gel electrolytes, *Membranes (Basel)*. 5 (2015) 810–823. <https://doi.org/10.3390/membranes5040810>.
- [50] S. Park, J.O. Baker, M.E. Himmel, P.A. Parilla, D.K. Johnson, Open Access RESEARCH Cellulose crystallinity index: measurement techniques and their impact on interpreting cellulase performance, 2010. <http://www.biotechnologyforbiofuels.com/content/3/1/10>.
- [51] H. Tang, H. Chen, B. Duan, A. Lu, L. Zhang, Swelling behaviors of superabsorbent chitin/carboxymethylcellulose hydrogels, *J Mater Sci.* 49 (2014) 2235–2242.  
<https://doi.org/10.1007/s10853-013-7918-0>.
- [52] A. Mıhranyan, K. Edsman, M. Strømme, Rheological properties of cellulose hydrogels prepared from *Cladophora* cellulose powder, *Food Hydrocoll.* 21 (2007) 267–272.  
<https://doi.org/10.1016/j.foodhyd.2006.04.003>.
- [53] S.Y. Ooi, I. Ahmad, M.C.I.M. Amin, Cellulose nanocrystals extracted from rice husks as a reinforcing material in gelatin hydrogels for use in controlled drug delivery systems, *Ind Crops Prod.* 93 (2016) 227–234. <https://doi.org/10.1016/j.indcrop.2015.11.082>.
- [54] Z. Jiang, X. Cao, Z. Li, L. Guo, Rheological behaviors and secondary networks of polyacrylamide hydrogel filled with silica, *J Pet Explor Prod Technol.* 6 (2016) 93–99.  
<https://doi.org/10.1007/s13202-015-0163-0>.
- [55] L.E. Beckett, J.T. Lewis, T.K. Tonge, L.S.T.J. Korley, Enhancement of the Mechanical Properties of Hydrogels with Continuous Fibrous Reinforcement, *ACS Biomater Sci Eng.* 6 (2020) 5453–5473. <https://doi.org/10.1021/acsbiomaterials.0c00911>.
- [56] M.M. Ghobashy, Superabsorbent, in: *Hydrogels*, InTech, 2018.  
<https://doi.org/10.5772/intechopen.74698>.
- [57] W.M. Cheng, X.M. Hu, D.M. Wang, G.H. Liu, Preparation and characteristics of corn straw-Co-AMPS-Co-AA superabsorbent hydrogel, *Polymers (Basel)*. 7 (2015) 2431–2445.  
<https://doi.org/10.3390/polym7111522>.
- [58] M. Shahzamani, S. Taheri, A. Roghanizad, N. Naseri, M. Dinari, Preparation and characterization of hydrogel nanocomposite based on nanocellulose and acrylic acid in the presence of urea, *Int J Biol Macromol.* 147 (2020) 187–193.  
<https://doi.org/10.1016/j.ijbiomac.2020.01.038>.
- [59] E.R. Kenawy, A. Hosny, K. Saad-Allah, Reducing nitrogen leaching while enhancing growth, yield performance and physiological traits of rice by the application of controlled-release urea fertilizer, *Paddy and Water Environment.* 19 (2021) 173–188.  
<https://doi.org/10.1007/s10333-020-00828-1>.
- [60] V. Champreda, W. Mhuantong, H. Lekakarn, B. Bunternngsook, P. Kanokratana, X.Q. Zhao, F. Zhang, H. Inoue, T. Fujii, L. Eurwilaichitr, Designing cellulolytic enzyme systems for biorefinery: From nature to application, *J Biosci Bioeng.* 128 (2019) 637–654.  
<https://doi.org/10.1016/j.jbiosc.2019.05.007>.

- [61] M.S. Ostrand, T.M. DeSutter, A.L.M. Daigh, R.F. Limb, D.D. Steele, Superabsorbent polymer characteristics, properties, and applications, *Agrosystems, Geosciences and Environment*. 3 (2020). <https://doi.org/10.1002/agg2.20074>.
- [62] P. Kaur, R. Agrawal, F.M. Pfeffer, R. Williams, H.B. Bohidar, *Hydrogels in Agriculture: Prospects and Challenges*, *J Polym Environ*. (2023). <https://doi.org/10.1007/s10924-023-02859-1>.
- [63] S.K. Patra, R. Poddar, M. Brestic, P.U. Acharjee, P. Bhattacharya, S. Sengupta, P. Pal, N. Bam, B. Biswas, V. Barek, P. Ondrisik, M. Skalicky, A. Hossain, *Prospects of Hydrogels in Agriculture for Enhancing Crop and Water Productivity under Water Deficit Condition*, *Int J Polym Sci. 2022* (2022). <https://doi.org/10.1155/2022/4914836>.
- [64] J.Y. Ye, W.H. Tian, C.W. Jin, *Nitrogen in plants: from nutrition to the modulation of abiotic stress adaptation*, *Stress Biology*. 2 (2022). <https://doi.org/10.1007/s44154-021-00030-1>.
- [65] F.F. Montesano, A. Parente, P. Santamaria, A. Sannino, F. Serio, *Biodegradable Superabsorbent Hydrogel Increases Water Retention Properties of Growing Media and Plant Growth*, *Agriculture and Agricultural Science Procedia*. 4 (2015) 451–458. <https://doi.org/10.1016/j.aaspro.2015.03.052>.
- [66] D. Khodadadi Dehkordi, *Evaluation of two types of superabsorbent polymer on soil water and some soil microbial properties*, *Paddy and Water Environment*. 16 (2018) 143–152. <https://doi.org/10.1007/s10333-017-0623-x>.
- [67] E.S. Abrisham, M. Jafari, A. Tavili, A. Rabii, M.A. Zare Chahoki, S. Zare, T. Egan, H. Yazdanshenas, D. Ghasemian, M. Tahmoures, *Effects of a super absorbent polymer on soil properties and plant growth for use in land reclamation*, *Arid Land Research and Management*. 32 (2018) 407–420. <https://doi.org/10.1080/15324982.2018.1506526>.
- [68] Y. Gao, X. Song, K. Liu, T. Li, W. Zheng, Y. Wang, Z. Liu, M. Zhang, Q. Chen, Z. Li, R. Li, L. Zheng, W. Liu, T. Miao, *Mixture of controlled-release and conventional urea fertilizer application changed soil aggregate stability, humic acid molecular composition, and maize nitrogen uptake*, *Science of the Total Environment*. 789 (2021). <https://doi.org/10.1016/j.scitotenv.2021.147778>.
- [69] S.A. Shahid, A.A. Qidwai, F. Anwar, I. Ullah, U. Rashid, *Improvement in the water retention characteristics of sandy loam soil using a newly synthesized poly(acrylamide-co-acrylic acid)/AlZnFe 2O 4 superabsorbent hydrogel nanocomposite material*, *Molecules*. 17 (2012) 9397–9412. <https://doi.org/10.3390/molecules17089397>.
- [70] P.C. Parvathy, A.N. Jyothi, K.S. John, J. Sreekumar, *Cassava Starch Based Superabsorbent Polymer as Soil Conditioner: Impact on Soil Physico-Chemical and Biological Properties and Plant Growth*, *Clean (Weinh)*. 42 (2014) 1610–1617. <https://doi.org/10.1002/clen.201300143>.